Role of Transverse Shock Waves on Deflagration-to-Detonation Transition in a Very Rough-walled Channel

G. Ciccarelli, C. Johansen, and M. Kellenberger
Queen's University
Kingston, Ontario, Canada

1 Introduction

Explosion front propagation in a channel is governed not only by the mixture transport properties, chemical kinetics and energy content but is also significantly affected by the surface roughness. Schelkin [1] was the first to show that flame acceleration can be enhanced by roughening the duct surface. Experiments have shown that a detonation in a very rough-walled channel can propagate at a velocity up to 50% lower than the theoretical Chapman-Jouget (CJ) [2]. Lee [2] has shown that this velocity deficit magnitude cannot solely be accounted for by momentum and heat losses to the wall. Lee proposed that for a very rough-walled channel scattering of the lead shock wave can produce a coupled shock-reaction front that propagates substantially slower than a CJ detonation wave. Such "low velocity detonation waves" or "quasi-detonations" were produced by Teodorcyk in a channel lined with cross-flow wires mounted on the top and bottom surface [3]. Lee proposed that the transverse waves produced by the interaction of the lead shock and the wall roughness maintains the coupling between the shock wave and the reaction zone even though they are very far apart [2].

In a horizontal channel partially filled with spherical beads rapid flame acceleration in the lower part of the channel containing the beads is followed by continued flame acceleration in the free space above the bead layer, herein referred to as the gap [4]. For conditions that did not result in transition to detonation, with gap heights of 76 mm and 107 mm, the maximum combustion front velocity was limited to the speed of sound of the combustion products [5]. For a smaller gap height of 38 mm, transition to detonation occurred at initial pressures greater than 30 kPa. For initial pressures of 15 and 20 kPa the front accelerated to velocities well in excess of the speed of sound of the combustion products but DDT was not observed [5]. The objective of the present series of experiments is to investigate the influence of the lower boundary condition on the flame and detonation propagation in the gap above the bead layer in a longer channel.

2 Experimental

Experiments were carried out in a modular 3.66 m long, 76 mm square horizontal channel where each module is 610 mm long. This is three times the total length of the channel used in the tests reported in [4]. The same optical module and single-pass schlieren system was used to obtain high – speed video of the explosion front propagation. Tests were performed with a mixture of CH_4+2(O_2+2/3N_2) at initial pressures in the range of 9 kPa to 15 kPa. The cell size for this mixture measured at 25 kPa in a 100 mm diameter tube is roughly160 mm. For all the initial pressures tested in this study the detonation cell size is significantly larger than the gap height and channel width. An automotive spark ignition system was used to ignite a flame at one end of the channel. The baseline test series was performed with 12.7 mm diameter ceramic beads filling roughly half the channel height, i.e., four layers of beads.

A series of tests was also performed with the last part of the bead layer replaced with a similar height solid piece of aluminum with a sharp leading edge. The sharp leading edge is located 2.1 m from the ignition end. The leading edge of the plate is sharp so as to minimize perturbations generated by the lead shock wave. In order to test the effect of surface roughness, experiments were performed with a single layer of beads placed on top of a shorter piece of aluminum maintaining the same height as the original bead layer, as shown in Fig. 1. In one series 12.7 mm beads were held in place by putty and in another 6.4 mm beads used by silicone. The putty and silicone also act as a filler to remove the cavities between the single bead layer and the plate.

3 Results

A baseline series of experiments was performed to characterize the flame propagation in the gap with the entire length of the channel half-filled with 12.7 mm beads. The explosion front velocity is plotted versus distance for different initial pressures in Fig. 2. Note there are two sets of data for each pressure condition obtained from instrumentation mounted on the top surface of the channel. The velocity data for the first 1.5 m was obtained from ionization probes, this data is re-plotted in subsequent figures for reference. The velocity data beyond 1.5 m was derived from pressure transducer shock wave time-of-arrival data. For initial pressures of 12 and 15 kPa what appears to be DDT occurs at roughly 1.8 m but the detonation subsequently fails because the detonation cell size is significantly larger than the gap height and channel width. At 9 kPa and 10 kPa DDT does not occur and the flame accelerates to a maximum velocity that is higher than the speed of sound in the combustion products (roughly 1030 m/s). For all four initial pressures, the flame velocity decreases towards the speed of sound of the combustion products towards the end of the channel. A similar trend is observed in the velocity based on ionization probe data.

High-speed shadowgraph video images taken of a DDT event for a 15 kPa test are shown in Fig. 3. The extent of the field-of-view is shown in the velocity plot in Fig. 2. The average shock speed over the four frames is 1638 m/s. In the first image a typical shock flame complex is observed above the bead layer, negligible light from reaction in the bead layer is detected. The shadowgraph images give an integrated view of the phenomenon, and since the gap is twice as wide as it is high, the reaction zone appears thicker than it is locally. In the second frame a local explosion is triggered at the bead layer surface, highlighted by a bright flash of light, a short distance behind the lead shock wave. The explosion front sweeps across the gap producing a bright spot at the point of reflection at the channel surface, see frame 3. In the same frame there is evidence of intense reaction in the bead layer associated with the explosion front. Light emitted in the bead layer outlines the oblique explosion front that was first reported in [4]. The reflected transverse wave propagating in the gap then impacts the bead layer surface in the fourth frame. During the time between frames 2 and 4 the inclination of the lead shock wave changes based on the position of the transverse shock wave.

The next two series of experiments were designed to investigate the propagation mechanism of the explosion front in the gap once it reaches a velocity greater than the speed of sound of the products. Specifically, the effect of the gap lower boundary, i.e., the bead layer upper surface which is characterized by its porosity and roughness, was investigated. The lower boundary porosity and surface roughness were removed by replacing the bead layer with a metal plate starting at 2.1 m. The explosion front velocity through the gap with the smooth surface plate in place is provided in Fig. 4. The velocities are obtained from both ionization probe and pressure transducer time-of-arrival data. Ionization probes were not used at the start of the plate in order to avoid perturbations generated by the electrodes. In general the explosion front velocity leading up to the plate was similar to that observed without the plate, see data in Fig. 2. The main difference in the velocity data is that with the plate present the velocity decreases to a lower velocity by the end of the channel, i.e., below 1000 m/s. The exception is the 15 kPa test where DDT occurs and the channel is too short for the front to decay below 1000 m/s.

Experiments were carried out with a single layer of beads placed on top of a shorter metal plate as shown in Fig. 1. This configuration removes the gap lower boundary porosity but retains the surface roughness. The explosion front velocity through the gap with a 12.7 mm diameter single-bead layer is provided in Fig. 5. The vertical bars represent the scatter in the data for multiple tests. For the 12 and 15 kPa tests, based on video results show a local explosion similar to that observed in Fig. 3, transition to detonation occurs and the front velocity only decreases marginally from the peak settling at a velocity well above 1500 m/s. This is significantly higher than the velocities observed for the full bead layer in Fig. 2 and the smooth plate in Fig. 4. The low velocity detonation, as described by Lee [2] is sustained by the transverse waves generated by the rough surface. These transverse are not produced with the smooth plate and are weakened by the expansion caused by the porosity of the full bead layer. For the 9 and 10 kPa tests the explosion front accelerates continuously from about 1100 m/s just before the start of the single bead layer at 2.1 m to about 1600 m/s at the end of the channel, a 24% CJ velocity deficit. A similar trend in the front velocity was observed for a single layer of 6.3 mm diameter beads, see Fig. 6, where the terminal velocity for all initial pressures is roughly 200 m/s higher than that observed for the single 12.7 mm diameter layer.

Shown in Fig. 7 are shadowgraph video images obtained at 9 kPa and 10 kPa showing the explosion front structure for the case of a full bead layer, smooth plate and a single 12.7 mm and 6.3 mm bead layer. The extent of the field-of-view is designated as FOV in the velocity plots in Figs. 5 and 6. For the full bead layer images in Fig. 7a, the transverse shock waves produced by the passage of the lead shock wave over the bead surface are clearly visible. There is visible separation between the shock wave and the leading edge of the turbulent flame brush. The front velocity is on the order of 1200 m/s which represents roughly the maximum velocity observed for the full bead layer, see Fig. 2. The flame brush appears symmetric despite the different top and bottom gap boundaries. For the smooth plate images in Fig. 7b, there is a large separation between the lead shock wave and the turbulent flame indicating a complete decoupling of the two. For the 12.7 mm single bead layer images in Fig. 7c, the explosion front structure appears very different than in the full bead layer in Fig. 7a. There is no clear flame leading edge and the reaction zone at the bottom of the gap is significantly shorter than at the smooth top surface. The shorter reaction zone next to the rough bottom surface is driven by the transverse shock waves (as discussed below) and not by enhanced shear generated turbulence. The wedge-shaped reaction zone and wrinkled appearance of the rear edge of the reaction zone indicates that direct shock ignition is not at play. This is supported by the long 9.5 ms induction time for a 1500 m/s shock wave calculated using the Konnov mechanism. For the 6.3 mm diameter bead layer images in Fig. 7d, the 9kPa test shows a similar wedge-shaped reaction zone front propagating at 1573m/s. However, for the 10 kPa test, where the front propagates at 2108 m/s, the reaction zone is of uniform length over the height of the gap. For a 2108 m/s shock the calculated induction time is 18 μs that corresponds to a 7.1 mm reaction zone length. The length of the reaction zone from the image, recall this is integrated over the width, is roughly two bead widths, or 12 mm.

For a steady one-dimensional shock flame structure the shock wave propagates at a higher velocity than the flame. In a very rough-walled channel scattering of the lead shock wave can produce a coupled shock-reaction front that propagates substantially slower than a CJ detonation wave. The velocity of the wave is controlled by the boundary condition and not the energy content of the mixture. Shock reflection off the rough-surface protrusions produce hot spots that can initiate reaction that spreads towards the center of the channel. For lower shock velocities, where autoignition due to shock reflection is not possible, vorticity production from the interaction of transverse shock waves and density gradients in the reaction zone results in a high turbulent burning rate. These mechanisms explain the shorter reaction zone near the bottom rough surface observed in Fig. 7. In a smooth-walled channel it is the piston action of the combustion products that limits the flame speed to the products speed of sound. In a very rough-walled channel it is the sidewall boundaries that drive the flame acceleration and thus it is not limited to the sonic back boundary. Once the front velocity is sufficiently fast there is a transition to a direct shock ignition mechanism, as in the 10 kPa test in Fig.

7d. As observed in Fig. 8 this transition can occur smoothly, i.e., without a local explosion, in a very rough-walled channel. Note how the reaction zone transitions from a wedge shape to uniform thickness without a dramatic change in front velocity.

4 Conclusions

The study has shown that it is possible to achieve a smooth transition from diffusion driven flame propagation to shock ignition driven detonation wave. It is proposed that flame acceleration past the speed of sound of the combustion products is possible in a very rough-walled channel because lead shock interactions with the rough surface can result in vorticity generation in the reaction zone and auto-ignition at hot spots on the wall.

References

[1] Shchelkin KI (1940). Zh. Eksp. Teor. Fiz. 10:823-827.

[2] Lee JH (2008). The Detonation Phenomenon, Cambridge University Press., ISBN 978-0-521-89723-5, p. 223.

[3] Teodorcyk A (1995). Fast deflagrations and detonations in obstacle-filled channels, Bulletin of Warsaw University of Technology, Number 79.

[4] Johansen C and Ciccarelli G (2009). Combustion in a horizontal channel partially filled with a porous media. Shock waves.

[5] Ciccarelli G, Hlouschko S, Johansen C, Karnesky J, Shepherd JE (2009). The study of geometric effects on the explosion front propagation in a horizontal channel with a layer of spherical beads, Proc. Comb. Inst. 32: 2299–2306.

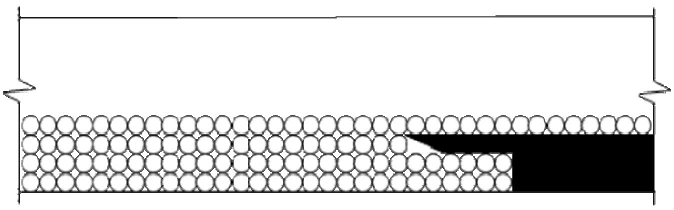

Figure 1. Schematic showing the transition from a four layer to a single layer of beads . The leading edge of the plate is located at 2.1 m from the ignition end of the channel.

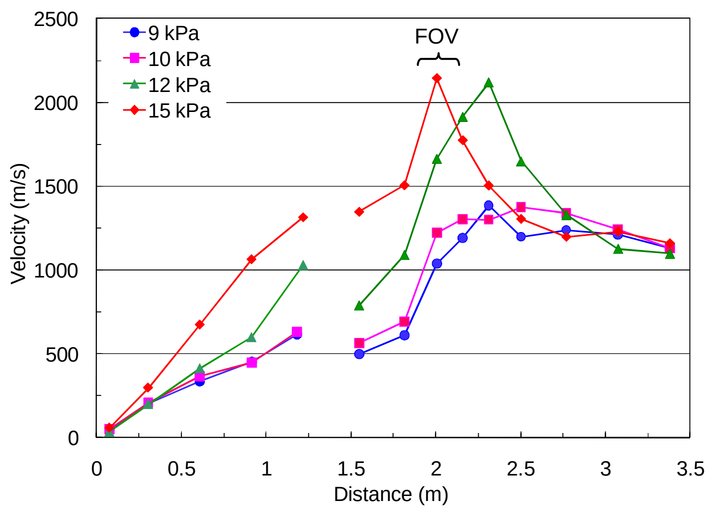

Figure 2. Explosion front velocity down the length of the channel, half-filled with 12.7 mm diameter beads, for different initial pressures Also shown is the field-of-view (FOV) for the images in Fig. 3.

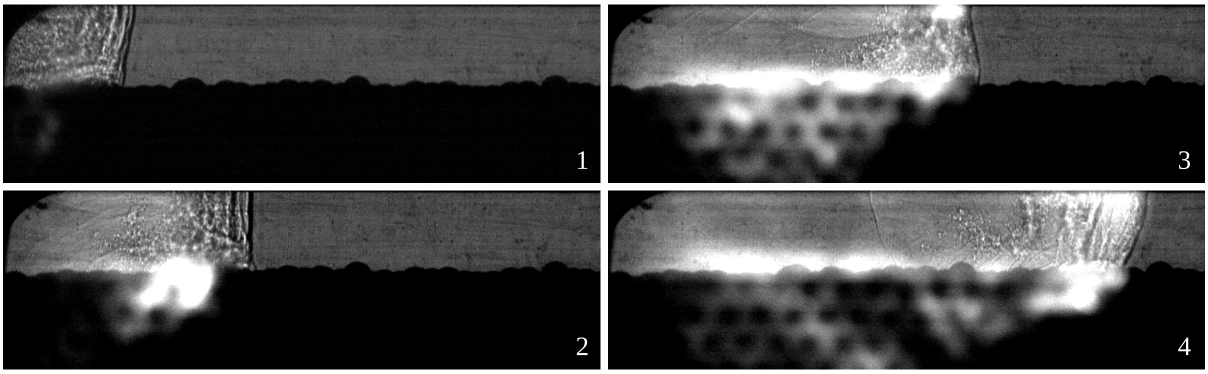

Figure 3. Shadowgraph video images showing DDT on surface of bead layer at 15 kPa (test 460). Left and right edge of field-of-view is 1.9 m and 2.1 m, respectively. Time between frames is 29 μs and the average front velocity over the four frames is 1638 m/s.

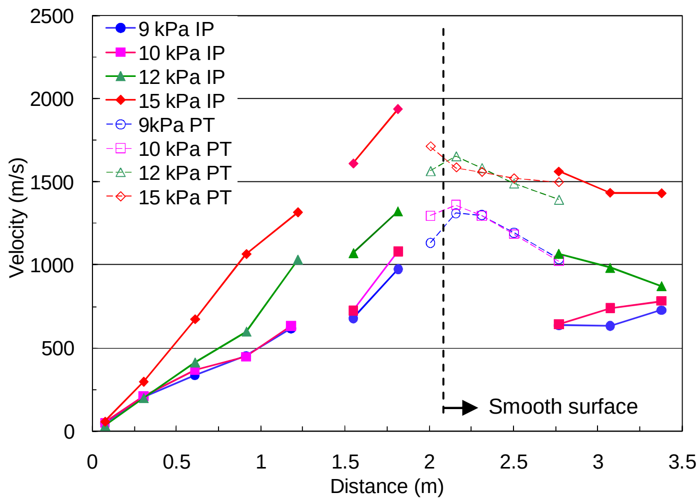

Figure 4. Explosion front velocity with a plate starting at 2.1 m. Solid symbols and lines correspond to ionization probe data, empty symbols and dotted lines correspond to pressure transducer data

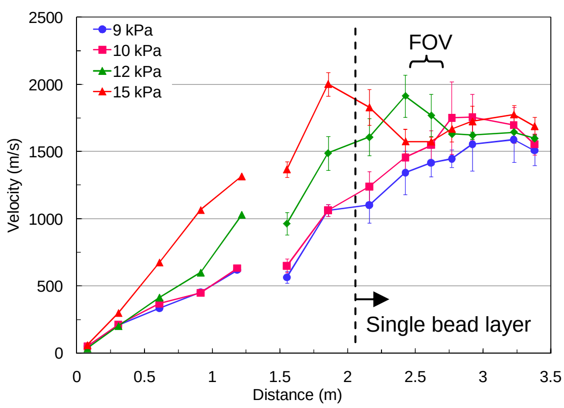

Figure 5. Explosion front velocity for a single layer of 12.7 mm beads starting at 2.1 m. Also shown is the field-of-view (FOV) for the images shown in Fig. 7.

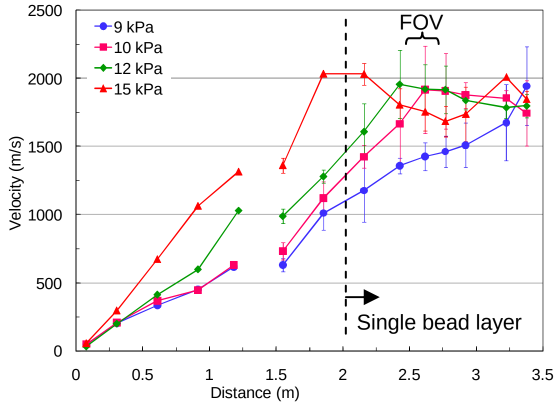

Figure 6. Explosion front velocity with a single layer of 6.3 mm beads starting at 2.1 m. Also shown is the field-of-view (FOV) for the images shown in Fig. 7.

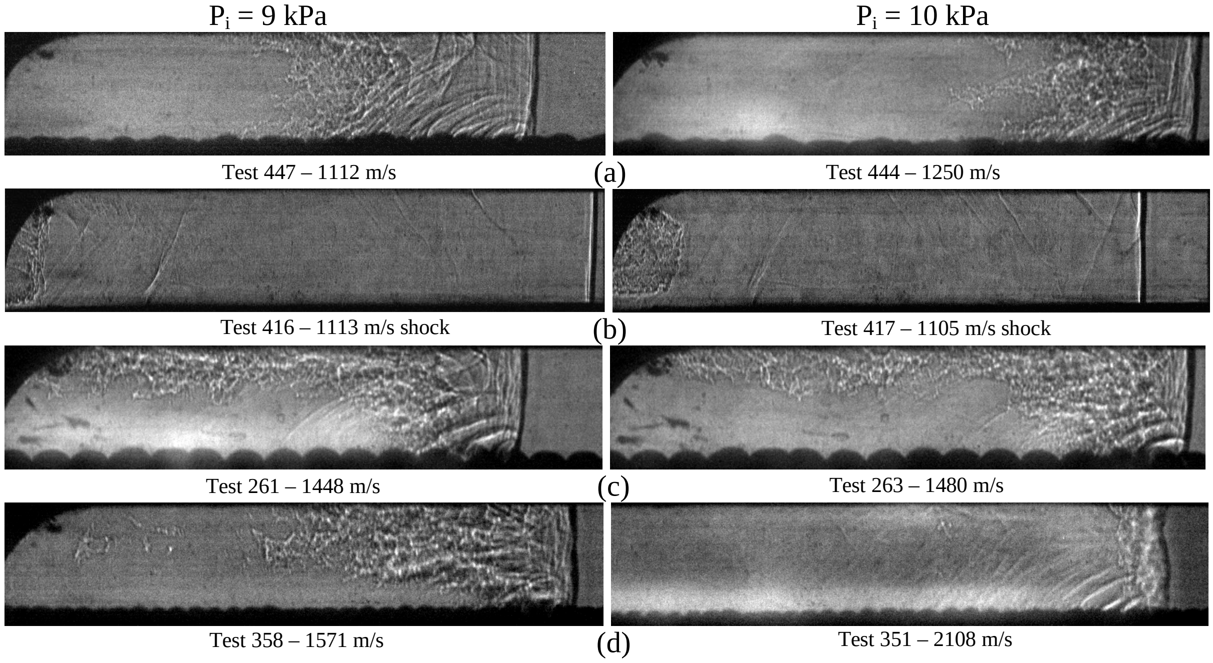

Figure 7. Shadowgraph video images showing explosion front structure (left column experiments are at 9 kPa and right column are at 10 kPa); a) continuous full bead layer, b) transition to smooth plate, c) transition to single layer of 12.7 mm beads, d) transition to single layer of 6.3 mm beads. Left and right edge of field-of-view is 2.5 m and 2.7 m, respectively. The average flame speed in the field-of-view is shown for each test.

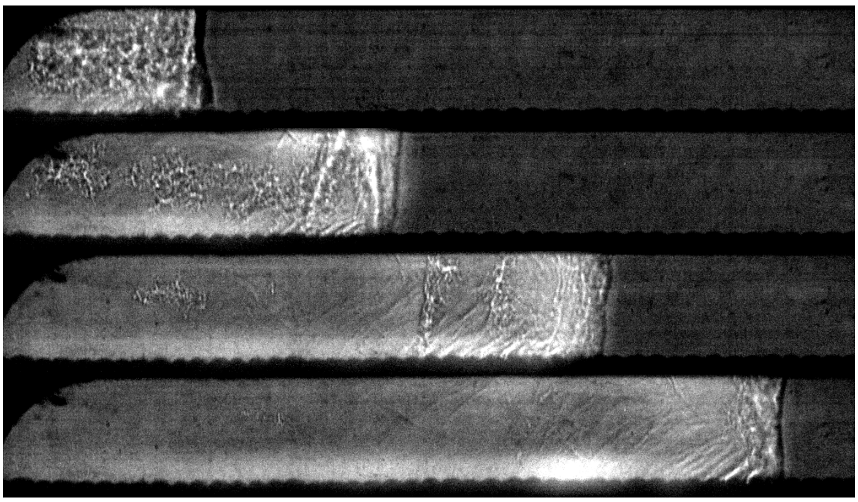

Figure 8. Shadowgraph video images showing the transition in the explosion front structure over a single layer of 6.3 mm beads at 10 kPa (test 347). Left and right edge of field-of-view is 2.5 m and 2.8 m, respectively. The average flame speed in the field-of-view is 2123 m/s, time between frames is 24 μs.